Praja1 ubiquitin ligase facilitates degradation of polyglutamine proteins and suppresses polyglutamine-mediated toxicity

Baijayanti Ghosh[a], Susnata Karmakar[b], Mohit Prasad[b], and Atin K. Mandal[a,*]
[a]Division of Molecular Medicine, Bose Institute, Kolkata 700054, India; [b]Department of Biological Sciences, Indian Institute of Science Education and Research Kolkata, Mohanpur, Nadia 741246, West Bengal, India

ABSTRACT **A network of chaperones and ubiquitin ligases sustain intracellular proteostasis and is integral in preventing aggregation of misfolded proteins associated with various neurodegenerative diseases. Using cell-based studies of polyglutamine (polyQ) diseases, spinocerebellar ataxia type 3 (SCA3) and Huntington's disease (HD), we aimed to identify crucial ubiquitin ligases that protect against polyQ aggregation. We report here that Praja1 (PJA1), a Ring-H2 ubiquitin ligase abundantly expressed in the brain, is diminished when polyQ repeat proteins (ataxin-3/huntingtin) are expressed in cells. PJA1 interacts with polyQ proteins and enhances their degradation, resulting in reduced aggregate formation. Down-regulation of PJA1 in neuronal cells increases polyQ protein levels vis-a-vis their aggregates, rendering the cells vulnerable to cytotoxic stress. Finally, PJA1 suppresses polyQ toxicity in yeast and rescues eye degeneration in a transgenic *Drosophila* model of SCA3. Thus, our findings establish PJA1 as a robust ubiquitin ligase of polyQ proteins and induction of which might serve as an alternative therapeutic strategy in handling cytotoxic polyQ aggregates.**

Monitoring Editor
James Olzmann
University of California, Berkeley

Received: Nov 24, 2020
Revised: Jun 7, 2021
Accepted: Jun 17, 2021

INTRODUCTION

Polyglutamine (polyQ) diseases are neurodegenerative disorders arising from CAG trinucleotide repeat expansion in the protein-coding region of the respective disease gene. Currently, nine such polyQ disorders have been identified: spinocerebellar ataxia (SCA) types 1, 2, 3, 6, 7, and 17; Huntington's disease (HD); dentatorubral pallidoluysian atrophy (DRPLA); and spinal and bulbar muscular atrophy (SBMA), which are progressive and dominantly inherited (except SBMA) (Zoghbi and Orr, 2000; Stoyas and La Spada, 2018). The most common among these neurodegenerative disorders with distinct pathological and clinical attributes, SCA3 and HD, are characterized by formation of amyloid-like toxic intracellular aggregates, which are hallmarks of all polyQ diseases. These insoluble intraneuronal aggregates and/or inclusions are formed at the cerebellar Purkinje neurons, brain stem, and spinocerebellar tracts and are caused as a result of a gain-of-function effect of polyQ expansion of the ataxin-3/huntingtin proteins causing neuronal dysfunction and death (Zoghbi and Orr, 2000; Paulson, 2012; Paulson *et al.*, 2017). These inclusions are immunoreactive for ubiquitin and sequester components of the ubiquitin proteasome system (UPS), molecular chaperones, and several transcription factors (Suhr *et al.*, 2001; Waelter *et al.*, 2001). The association of polyQ aggregates with the components of the protein quality control (PQC) machinery induces cellular response to manage the accumulation of misfolded proteins either by refolding them by molecular chaperones or degrading them by the degradation machinery. Multiple lines of evidence have demonstrated the function of selective molecular chaperones, the proteasome system, and autophagy in suppression of aggregate formation and modulation of polyQ pathogenesis (Chai *et al.*, 1999; Brehme *et al.*, 2014; Djajadikerta *et al.*, 2020).

Cellular proteostasis is finely orchestrated by the two arms of the PQC system: molecular chaperones and degradation machinery. Apart from their role in protein folding, chaperones hand over misfolded proteins to ubiquitin ligases for tagging them with ubiquitin for their degradation via the proteasome or autophagic pathway. The presence of approximately 600 ubiquitin ligases in the

This article was published online ahead of print in MBoC in Press (http://www.molbiolcell.org/cgi/doi/10.1091/mbc.E20-11-0747) on June 23, 2021.

Conflict of interest: The authors declare no conflict of interest.

*Address correspondence to: Atin K. Mandal (mandalak@jcbose.ac.in).

Abbreviations used: AD, Alzheimer's disease; CHIP, carboxy-terminus of Hsp70-interacting protein; HD, Huntington's disease; PD, Parkinson's disease; PJA1, Praja1; polyQ, polyglutamine; PQC, protein quality control; SCA3, spinocerebellar ataxia type 3.

mammalian system (Deshaies and Joazeiro, 2009) suggests a cohort of ubiquitin ligases laboring in unison to protect cells from accumulation of misfolded proteins and their aggregates and subsequent cytotoxic stress (Theodoraki *et al.*, 2012; Kuang *et al.*, 2013). PolyQ-expanded ataxin-3 and huntingtin are similarly degraded by multiple ubiquitin ligases, such as the carboxy-terminus of Hsp70-interacting protein (CHIP), which promotes degradation of polyQ proteins and reduces their aggregation in cell and animal models of SCA3 and HD (Jana *et al.*, 2005; Miller *et al.*, 2005). Endoplasmic reticulum–associated E3 ubiquitin ligase autocrine motility factor receptor (AMFR) or Gp78 and E6-associated protein (E6-AP) provides cytoprotection against mutant SOD1 and mutant ataxin-3–mediated toxicity (Ying *et al.*, 2009; Mishra *et al.*, 2013). Parkin is impaired in Parkinson's disease (PD) and interacts with expanded polyQ proteins and promotes their degradation (Tsai *et al.*, 2003). Recent studies also establish the role of Mahogunin RING finger-1 (MGRN1) and Itchy E3 ubiquitin ligase (ITCH) in promoting the degradation of expanded polyQ proteins and suppression of polyQ-mediated toxicity (Chhangani and Mishra, 2013; Chhangani *et al.*, 2014). Because polyQ disorders are age-onset neurodegenerative disorders where the cellular machinery eventually loses the robustness and efficiency of the PQC, stimulating the components of the PQC has been commonly used as a therapeutic strategy to ameliorate the pathogenesis of these disorders. Interestingly, ataxin-3 is a deubiquitinating enzyme (DUB) that tightly regulates the activity of CHIP and Parkin, E3 partners of ataxin-3 (Durcan and Fon, 2011, 2013; Durcan *et al.*, 2011; Scaglione *et al.*, 2011). Moreover, reduced levels of CHIP and Parkin in mouse models of SCA3 imply the involvement of other robust E3 ligases restricting disease pathogenesis (Durcan and Fon, 2011; Durcan *et al.*, 2011; Scaglione *et al.*, 2011).

Analyzing the interactome of ataxin-3 protein by String 9.0 and BIOGRID databases, we came across a particular ubiquitin ligase, Praja1 (PJA1), a RING-H2 ubiquitin ligase that had predictive interaction with ataxin-3, but its function was unknown. PJA1 is expressed ubiquitously in various tissues, although the highest expression is observed in the brain. Interestingly, the PJA1 gene is located in a specific region of the X-chromosome, which is associated with numerous X-linked cognitive disorders, and a contiguous gene deletion results in craniofrontonasal disorder (Mishra *et al.*, 1997; Wieland *et al.*, 2007). Moreover, a loss-of-function PJA1 variant was linked to neurodevelopmental disorders associated with epilepsy or/and craniofacial abnormalities (Suzuki *et al.*, 2020). Notably, among 29 other genes (linked to neurodegenerative disorders) the PJA1 gene is down-regulated in PR5 mutant Tau transgenic mice (Alzheimer's disease [AD]) amygdala (Ke *et al.*, 2012). In several other studies, PJA1 has been shown to be differentially regulated in a HD mouse model, amyloid precursor protein (APP)-treated organotypic hippocampal slice cultures, and the bipolar disorder-affected orbitofrontal cortex (Stein *et al.*, 2004; Cui *et al.*, 2006; Ryan *et al.*, 2006). In a recent study, PJA1 has also been shown to suppress cytoplasmic TDP-43 inclusions (Watabe *et al.*, 2020).

We report here that PJA1 acts as an ubiquitin ligase of polyQ proteins, ataxin-3 and huntingtin, and inhibits their accumulation as toxic aggregates. Thereby, PJA1 suppresses polyQ-mediated toxicity in yeast and a *Drosophila* SCA3 transgenic model. Additionally, PJA1 silencing in mouse neuronal cells shows a marked increase in SCA3 and HD aggregates, indicating the crucial role of PJA1 in disease pathogenesis when its function is compromised at old age. Thus, we demonstrate PJA1's function as a critical ubiquitin ligase present in the brain, the levels of which can be manipulated to strategize a potential therapy against polyQ disorders in general.

RESULTS

PJA1 is dysregulated by polyQ proteins, ataxin-3 and huntingtin

Reduced efficiency of PQC machinery leads to the development of age-onset neurodegenerative disorders that result in the accumulation of terminally misfolded toxic proteins (Bence *et al.*, 2001; Bennett *et al.*, 2005; Thibaudeau *et al.*, 2018). For instance, Ubiquitin ligases, viz., MGRN1, CHIP, and Parkin, levels and their functions are compromised in neurodegenerative diseases including polyQ disorders such as SCA3 and HD (Durcan and Fon, 2011, 2013; Durcan *et al.*, 2011; Scaglione *et al.*, 2011; Chhangani and Mishra, 2013). Because PJA1 ubiquitin ligase is highly enriched in brain tissue including regions of the cerebellum, cerebral cortex, medulla, occipital lobe, frontal temporal lobe, and the putamen (Yu *et al.*, 2002), we speculated that its level might be reduced in neurodegeneration and result in the accumulation of misfolded polyQ proteins. To check our hypothesis, we examined the level of endogenous PJA1 upon overexpression of polyQ-expanded proteins ataxin-3 and huntingtin in mouse neuroblastoma Neuro2A (N2A) cells. Truncated 20Q and 80Q ataxin-3 in pEGFP-N1 (henceforth 20QT and 80QT) and N-terminal fragment of HTT 16Q in the pEGFP-C1 and 83Q in the pDsRed (16Q HTT and 83Q HTT) vector and the corresponding empty vectors were transfected in N2A cells, and PJA1 transcripts were analyzed. Interestingly, the mRNA levels of PJA1 in both ataxin-3 (20QT and 80QT) and huntingtin (16Q and 83Q)-overexpressed N2A cells were decreased by approximately 0.6- and 0.5-fold, respectively, as compared with control cells (Figure 1, A and C). However, no reduction of PJA1 transcripts was noticed in the case of empty vectors. The reduction in the mRNA transcripts was also reflected in the endogenous protein levels of PJA1 in both ataxin-3 and huntingtin overexpressed N2A cells (Figure 1, B and D). The diminution of PJA1 levels during polyQ disorders is consistent with the decline in its levels in PR5 mutant Tau transgenic mice amygdala, bipolar disorder–affected orbitofrontal cortex, and other cognitive disorders (Stein *et al.*, 2004; Cui *et al.*, 2006; Ryan *et al.*, 2006; Wieland *et al.*, 2007).

PJA1 interacts with normal and polyQ-expanded proteins and colocalizes with polyQ aggregates

Because overexpression of polyQ-expanded proteins leads to a marked reduction in PJA1 levels, we hypothesized a physical interaction between PJA1 ubiquitin ligase and polyQ proteins. Intracellular aggregates tend to sequester several proteins, including chaperones, ubiquitin ligases, and proteasomal subunits (Stenoien *et al.*, 1999). Hence, we inspected whether PJA1 was recruited to the aggregates formed by the polyQ proteins. To investigate that, DsRed-PJA1 was cotransfected with green fluorescent protein (GFP)-tagged ataxin-3 constructs in HEK293T cells. Expression of polyQ-expanded ataxin-3 (80QT and 130QF) shows large cytoplasmic aggregates, and these aggregates indubitably associated with PJA1 as observed by confocal microscopy (Figure 2, A and B). However, small aggregates of 20QT ataxin-3 were observed in very few cells, which also colocalized with PJA1 (Figure 2C). Likewise, polyQ-expanded huntingtin (83Q HTT) aggregates colocalized with PJA1 (Figure 2Dii).

Predictive interactions between PJA1 and ataxin-3 were also indicated by in silico studies using STRING and BIOGRID databases. To ascertain the interaction between PJA1 ubiquitin ligase and ataxin-3 proteins, coimmunoprecipitation was next performed with GFP-ataxin-3 and HA-PJA1. To rule out the nonspecific interaction with GFP and PJA1, an initial control experiment was carried out by immunoprecipitating GFP and then probing for PJA1 or vice versa

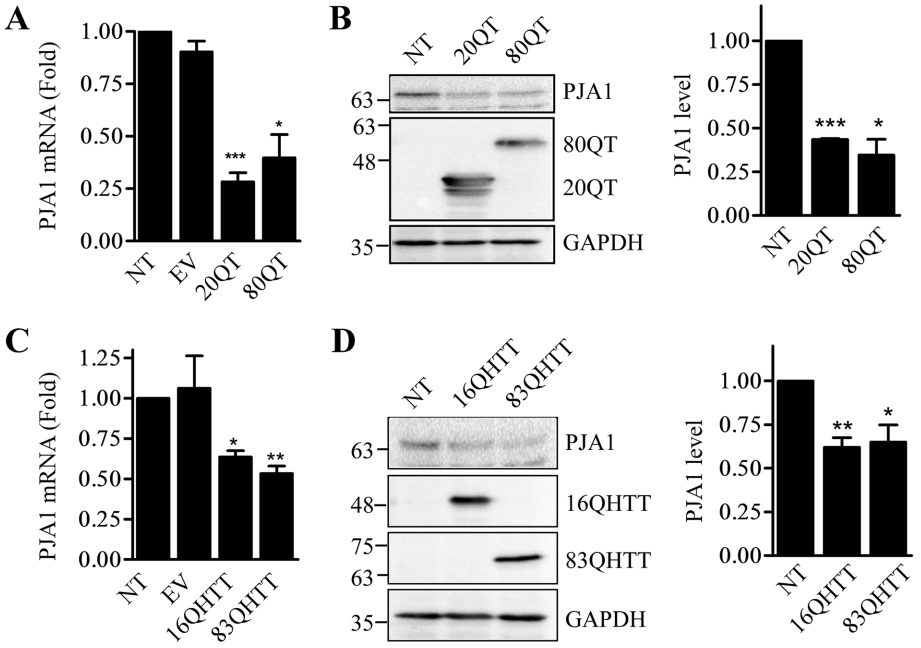

FIGURE 1: PJA1 is dysregulated by polyQ proteins. (A. C) PJA1 transcript level was decreased upon overexpression of ataxin-3 and huntingtin protein. Normal and polyQ-expanded ataxin-3 (A) and huntingtin (C) plasmids and their corresponding empty vectors pEGFP-C1 and pDsRed-C1 were transfected in N2A cells. Seventy-two hours after transfection, total RNA was isolated from the cells and subjected to quantitative RT-PCR. Data were collected from three separate experiments and normalized to the levels of GAPDH. Values are the mean ± SD. Significance of the data was calculated by *t* test. * $p < 0.05$, ** $p < 0.01$, *** $p < 0.001$ compared with nontransfected cells. (B, D) PJA1 protein level is reduced in ataxin-3 and huntingtin transformed cells. The lysates from A and C overexpressing ataxin-3 and huntingtin, respectively, were immunoblotted with PJA1 and GAPDH antibody. Lysate shows the expression of ataxin-3 and huntingtin protein by GFP and DsRed antibody. The bands were quantified, normalized with GAPDH, and plotted as bar diagrams. Error bar represents SD of three independent experiments. Significance was calculated by *t* test. * $p < 0.05$, ** $p < 0.01$, *** $p < 0.001$. NT stands for nontransfected cells.

in HEK293T cells. No interaction was observed between GFP protein expressed from empty vector and PJA1 (Supplemental Figure S1C). Subsequently, coimmunoprecipitation was carried out by immunoprecipitating PJA1 and probing for ataxin-3 or vice versa in both HEK293T cells (Figure 3A and Supplemental Figure S1A) and N2A cells (Supplemental Figure S1, D and E). Robust interaction not only with normal ataxin-3 protein but also with 80QT or full-length 130Q protein was observed with PJA1. Moreover, to further confirm the specificity of interaction between PJA1 and ataxin-3, we performed coimmunoprecipitation experiments between overexpressed PJA1, RING domain–deleted PJA1, and endogenous ataxin-3 in HEK293T cells by immunoprecipitating ataxin-3 (Figure 3D). Interaction between endogenous ataxin-3 with PJA1, but not with its RING deletion counterpart, was observed, indicating specificity of association of PJA1 and ataxin-3. Experiments checking the interaction between PJA1 with another polyQ protein, huntingtin, also produced similar results. PJA1 coimmunoprecipitated with normal (16Q HTT) and polyQ-expanded (83Q HTT) huntingtin proteins, and not with GFP and DsRed protein expressed from the respective empty vectors (Figure 3, B and C, and Supplemental Figure S1B).

PJA1 suppresses formation of polyQ-expanded aggregates

PJA1 is a Ring-H2 finger ubiquitin ligase abundantly expressed in the brain (Yu *et al.*, 2002). With its RING finger motif, it promotes degradation of MAGED1 and EZH2 proteins by the ubiquitin proteasome system (Sasaki *et al.*, 2002; Consalvi *et al.*, 2017). PJA1 induces learning in the basolateral amygdala during formation of fear memory, which is in agreement with a study establishing the role of PJA1 in cognitive disorders like X-linked mental retardation (Stork *et al.*, 2001; Yu *et al.*, 2002). One prominent clinical manifestation of polyQ disorders is cognitive defect (Gardiner *et al.*, 2019), which could be due to dysregulation of PJA1 ultimately leading to the toxic accumulation of misfolded polyQ proteins. To examine whether PJA1 can mobilize polyQ aggregates, we checked the formation of ataxin-3 (80QT/130QF) aggregates upon ectopic expression of PJA1 in HEK293T cells by fluorescence microscopy. We noticed a 60–70% reduction in the number of 80QT and 130QF (Figure 4Ai) aggregates counted per 100 GFP-positive cells coexpressing ataxin-3 and PJA1. A similar result was obtained for 83QHTT when PJA1 was overexpressed (Figure 4C). Notably, reduced overall fluorescence intensity of 16QHTT was observed in the PJA1-expressing condition. These data were further supported by decreased levels of ataxin-3 (Figure 4Aii) and huntingtin proteins as seen in the Western blot analysis (Figure 4Ciii). The above results suggest a probable role of PJA1 in mediating degradation of polyQ proteins by utilizing its ubiquitin ligase activity. To confirm that possibility, we deleted the RING finger motif of PJA1 or mutated its conserved His residue (H553) to Ser and checked its capacity to reduce ataxin-3 aggregates. Our result showed that RING-deleted PJA1 was unable to reduce 80QT ataxin-3 aggregates and its protein level, whereas RING mutant (H553S) PJA1 was able to reduce the same, although to a lesser extent in comparison to wild-type (WT) PJA1 (Figure 4B). This observation suggests that reduction of polyQ aggregates is linked with PJA1 ubiquitin ligase activity mediated by its RING finger motif.

To further confirm PJA1-driven reduction of polyQ aggregates, we used baker's yeast *Saccharomyces cerevisiae*, which is devoid of both the proteins. Being a eukaryote, *S. cerevisiae* serves as an effective model and is widely used for many protein misfolding diseases, including neurodegenerative diseases (Miller-Fleming *et al.*, 2008). We cloned ataxin-3 and PJA1 in yeast under galactose- and copper-inducible promoters, respectively. PJA1 expression was promoted by the addition of 300 μM copper before ataxin-3 expression with 2% galactose. The status of the ataxin-3 aggregates was then checked by fluorescence microscopy. We noticed an overall decrease in the number of ataxin-3 aggregates in yeast cells expressing PJA1 which was further supported by a significant reduction in the protein level as well (Supplemental Figure S2). Furthermore, a reduction of the endogenous level of ataxin-3 protein was observed upon PJA1 expression in HEK293 cells (Figure 4D). On the contrary, when endogenous PJA1 was silenced using short hairpin RNA (shRNA) targeted to PJA1 (as shown by real-time [RT]-PCR due to poor sensitivity in detecting endogenous PJA1 with antibody)

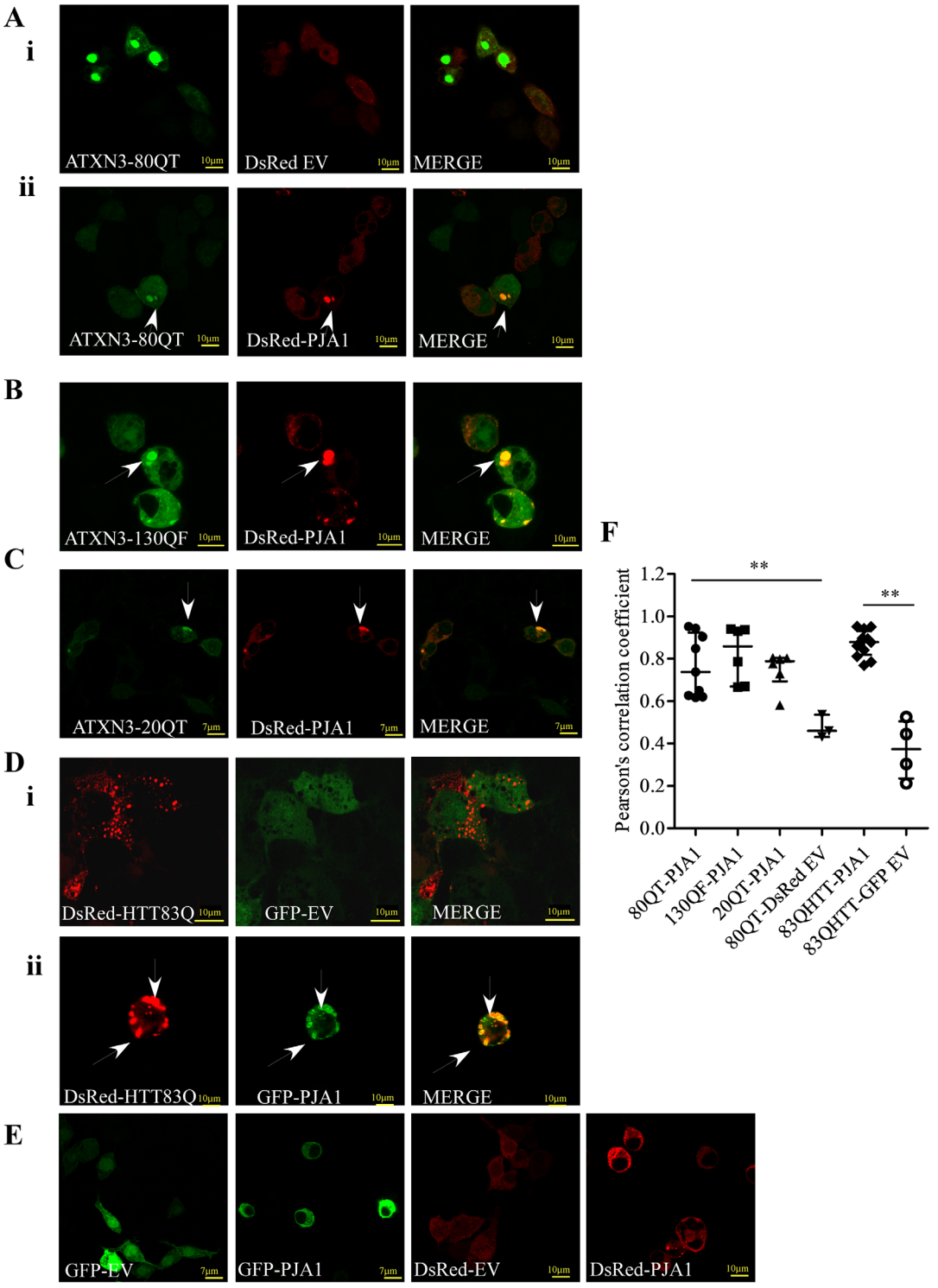

FIGURE 2: PJA1 colocalizes with polyQ aggregates. (A–C) Colocalization of PJA1 with ataxin-3. PJA1 cloned in the pDsRed vector was cotransfected with 80QT (Aii), 130QF (B), and 20QT (C) ataxin-3 in HEK293T cells. Cells were processed as described in *Materials and Methods* for visualization under a confocal microscope. Arrows indicate the recruitment of PJA1 to ataxin-3 aggregates. (D) PJA1 colocalizes with 83QHTT aggregate. PJA1 cloned in the pEGFP-C1 vector was transiently transfected with pDsRed-83QHTT in HEK293T cells. At 24 h, cells were processed for confocal microscopy. Colocalization of PJA1 with HTT aggregates is indicated. (E) pEGFP-C1/pDsRed empty vector (EV) and PJA1 alone showed diffused localization in HEK293T cells. (F) Pearson's correlation coefficients for colocalization between polyQ proteins and PJA1. The plot depicts Pearson's correlation coefficients for colocalization analysis. The *Rp* values for 20QT and PJA1 (0.78, Interquartile range [IQR] 0.6–0.8), 80QT and PJA1 (0.77, IQR 0.62–0.95), 130QF and PJA1 (0.86, IQR 0.67–0.94), 83QHTT and PJA1 (0.88, IQR 0.62–0.95), 80QT and DsRed (0.46, IQR 0.43–0.53), and 83QHTT and GFP (0.36, IQR 0.20–0.52) indicate the extent of colocalization of polyQ proteins and PJA1 and show that PJA1 and polyQ proteins significantly colocalized with each other. Significance was calculated by *t* test. ** $p < 0.01$.

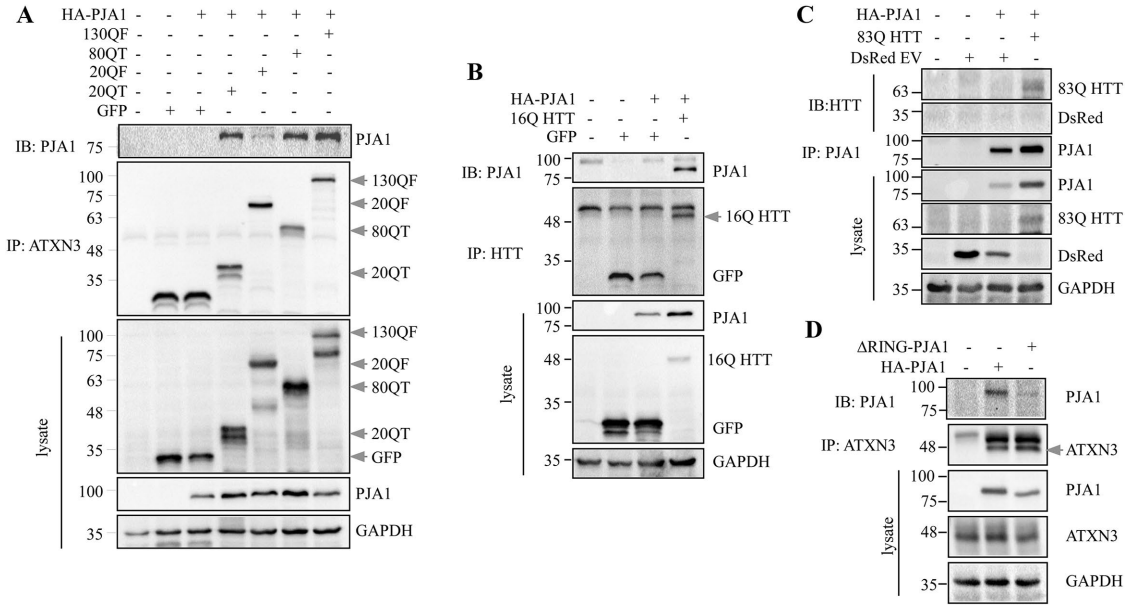

FIGURE 3: PJA1 interacts with normal and polyQ-expanded proteins. (A) PJA1 interacts with ataxin-3 proteins. (A) 20Q truncated (20QT), 20Q full-length (20QF), 80Q truncated (80QT), and 130Q full-length (130QF) ataxin-3 in the pEGFP-N1 vector were cotransfected with HA-tagged PJA1 (pCMV-HA-PJA1) in HEK293T cells. Twenty-four hours after transfection, cells were lysed and subjected to immunoprecipitation with anti-GFP antibody. The blots were consecutively probed with anti-HA and anti-GFP antibody for detection of PJA1 and ataxin-3, respectively. The total lysate shows the expression of the respective proteins. (B, C) PJA1 interacts with huntingtin protein. N-terminal fragments of 16Q huntingtin (16QHTT) protein in the pEGFP-C1 vector (B) and 83QHTT in the pDsRed vector (C) were cotransfected with HA-PJA1 in HEK293T cells. Cells were harvested and processed for immunoprecipitation with anti-GFP (B) and anti-HA (C) antibodies. The blots were successively probed with anti-GFP/anti-DsRed and anti-HA antibodies. (D) PJA1 interacts with endogenous ataxin-3 protein. HA-tagged PJA1 and ΔRING-PJA1 were transfected in HEK293T cells. Twenty-four hours after transfection, cells were lysed and subjected to immunoprecipitation using anti-SCA3 antibody. The blots were consecutively probed with respective antibodies. The total lysate shows the expression of the respective proteins. GAPDH is the loading control for all the experiments. Results are representative of three independent experiments.

(Figure 5A) in N2A cells overexpressing normal and polyQ-expanded ataxin-3, an approximately five- to six-fold increment in protein levels of the respective ataxin-3 proteins was detected (Figure 5B). The knockdown of endogenous PJA1 levels also resulted in a significant increase in the number of polyQ-expanded ataxin-3/huntingtin aggregates (Figure 5, C and D). Similar results were obtained by using small interfering RNA (siRNA) targeted to PJA1 in N2A cells (Figure 5, E–G). Silencing of PJA1 enhances 20QT and 80QT ataxin-3 protein levels as seen by Western blot analysis and also by fluorescence microscopy. Altogether, these results suggest that PJA1 modulates polyQ proteins and their aggregates by utilizing its ubiquitin ligase activity.

PJA1 facilitates degradation of wild-type and polyQ-expanded ataxin-3 by promoting ubiquitination

On the basis of previous reports of substrate degradation by PJA1 ubiquitin ligase (Sasaki *et al.*, 2002; Consalvi *et al.*, 2017) and diminution of steady state expression of ataxin-3 and huntingtin proteins in mammalian and yeast cells in the presence of PJA1 (Figure 4, A, C, and D), we wanted to investigate whether PJA1 aided in the degradation of polyQ proteins. Moreover, the unaltered endogenous ataxin-3 mRNA level in PJA1-overexpressed cells ruled out possible transcriptional down-regulation of ataxin-3 by PJA1 (Supplemental Figure S3), which further supports PJA1's function in reducing ataxin-3 at the posttranslational level. Tracking the turnover of polyQ proteins in mammalian cells was not pursued as PJA1 is a short-lived protein promoting self-ubiquitination (Zoabi *et al.*, 2011). Instead, substitute experiments in mammalian cells (N2A) were performed wherein PJA1 was overexpressed in ascending concentrations and ataxin-3 was found to be reduced in a concentration-dependent manner (Figure 6, A and B). Furthermore, temporal expression of PJA1 showed a gradual decrease in ataxin-3 protein levels over time (Figure 6C). These results suggest a correlation between PJA1 overexpression and reduction of ataxin-3 level. To confirm this, we pursued a galactose shutoff chase of 80QT ataxin-3 in a yeast system upon expression of PJA1 from an inducible copper promoter. Enhanced turnover of ataxin-3 was observed until 4 h of chase when adequate amount of PJA1 is present, which suggests PJA1-mediated degradation of ataxin-3 (Figure 6D). Furthermore, stabilization of 80QT ataxin-3 was observed in cycloheximide chase upon silencing of PJA1 in N2A cells (Figure 6E).

Because degradation is accompanied by tagging substrate molecules with ubiquitin moieties by ubiquitin ligase, we next assessed whether PJA1 was capable of ubiquitinylating ataxin-3 in a yeast system. We noticed an increased ubiquitination of 80QT ataxin-3 when PJA1 was expressed in yeast cells from a copper-inducible promoter (Figure 6F). Similarly, ubiquitination of 20QT ataxin-3 was drastically increased in *atg8* knockout yeast cells expressing PJA1 (Figure 6G). On the contrary, silencing of PJA1 by shRNA or siRNA (validated by RT-PCR) targeted to PJA1 reduces polyubiquitination of 80QT ataxin-3 in N2A cells (Figure 6H). Together, these results corroborate the fact that PJA1 is an E3 ubiquitin ligase that ubiquitinates ataxin-3 and hence promotes its degradation.

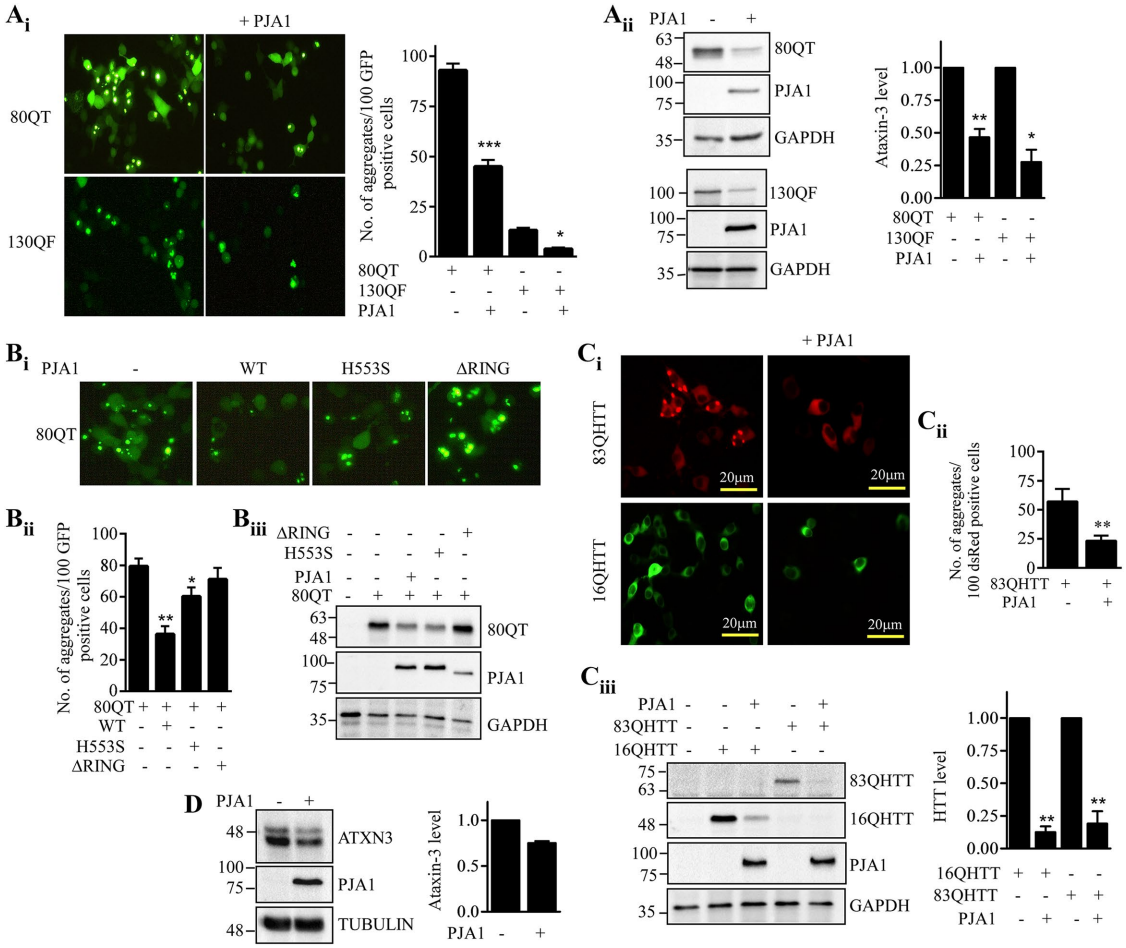

FIGURE 4: PJA1 suppresses the formation of polyQ-expanded aggregates. (A) PJA1 reduces ataxin-3 aggregates. (i) HA-tagged PJA1 and the corresponding empty vector were transfected with 80QT and 130QF ataxin-3 into HEK293T cells. Transfected cells were viewed under fluorescence microscope. Aggregates were counted per 100 GFP-positive cells from 10 fields randomly chosen and plotted in a bar graph. Values are the mean ± SD. Significance was calculated by *t* test. * $p < 0.05$, *** $p < 0.001$. (ii) The lysates from i were subjected to immunoblotting with anti-GFP and anti-HA antibodies for detection of ataxin-3 and PJA1, respectively. The bands were quantified, normalized with GAPDH, and plotted as bar diagrams. Error bar represents SD of three independent experiments. Significance was calculated by *t* test. *, ** $p < 0.05$ and $p < 0.01$, respectively. (B) Impaired PJA1 is unable to suppress aggregation of ataxin-3. 80QT ataxin-3 was transfected alone or in combination with WT, H553S, and ΔRING-PJA1 in HEK293T cells. Formation of ataxin-3 aggregates was viewed under a fluorescence microscope (i). The aggregates were counted as described earlier, and the quantification was plotted in a bar graph (ii). *, ** $p < 0.05$ and $p < 0.01$, respectively. The same cells were subjected to immunoblotting with anti-GFP, anti-HA, and anti-GAPDH antibodies for expression of the corresponding proteins (iii). (C) PJA1 reduces the aggregation of HTT protein. HA-PJA1 was transfected with pDsRed-83QHTT/ pEGFP-C1-16QHTT in HEK293T cells (i). The 83QHTT aggregates were quantified and plotted as a bar diagram (ii). Error bar represents SD, $p < 0.01$. Western blot analysis shows the expression of the respective protein in cell lysates with anti-GFP, anti-DsRed, and anti-HA antibodies (iii). GAPDH serves as loading control. The bands were quantified, normalized with GAPDH, and plotted as a bar diagram. Error bar represents SD of three independent experiments. Significance was calculated by *t* test. $p < 0.01$. (D) PJA1 reduces endogenous ataxin-3 levels. PJA1 was transfected into HEK293 cells. Cell lysates were subjected to Western blotting, and endogenous ataxin-3 was detected with anti-SCA3 1H9 antibody. Tubulin was used as the loading control. The bar diagram was plotted from band intensities calculated and normalized with loading control from two independent experiments.

Ubiquitin ligase–mediated clearance of protein aggregates is powered preferentially by the autophagy pathway (Nixon, 2013). Previously PJA1 function has been shown in degradation of MAGED1 and EZH2 proteins by the UPS (Sasaki *et al.*, 2002; Consalvi *et al.*, 2017). Aligning this result, we also found rescue of EZH2 protein upon inhibition of proteasome by lactacystin in PJA1-expressing HEK293T cells (Figure 7A). Here, we wanted to check whether PJA1 shuttles ubiquitinated polyQ proteins via UPS or autophagy. Interestingly, PJA1-mediated reduction of ataxin-3 protein was rescued when the proteasome or autophagy pathway is blocked (Figure 7, B and C). This result suggests proteasomal as well as autophagic clearance of ataxin-3 facilitated by PJA1. To further validate autophagy-mediated degradation of ataxin-3 by PJA1, yeast knockout strain *atg8*Δ was used. Levels of 20QT ataxin-3 were restored in *atg8*Δ cells, confirming the role of PJA1 in promoting degradation of ataxin-3 also through the autophagy pathway (Figure 7D).

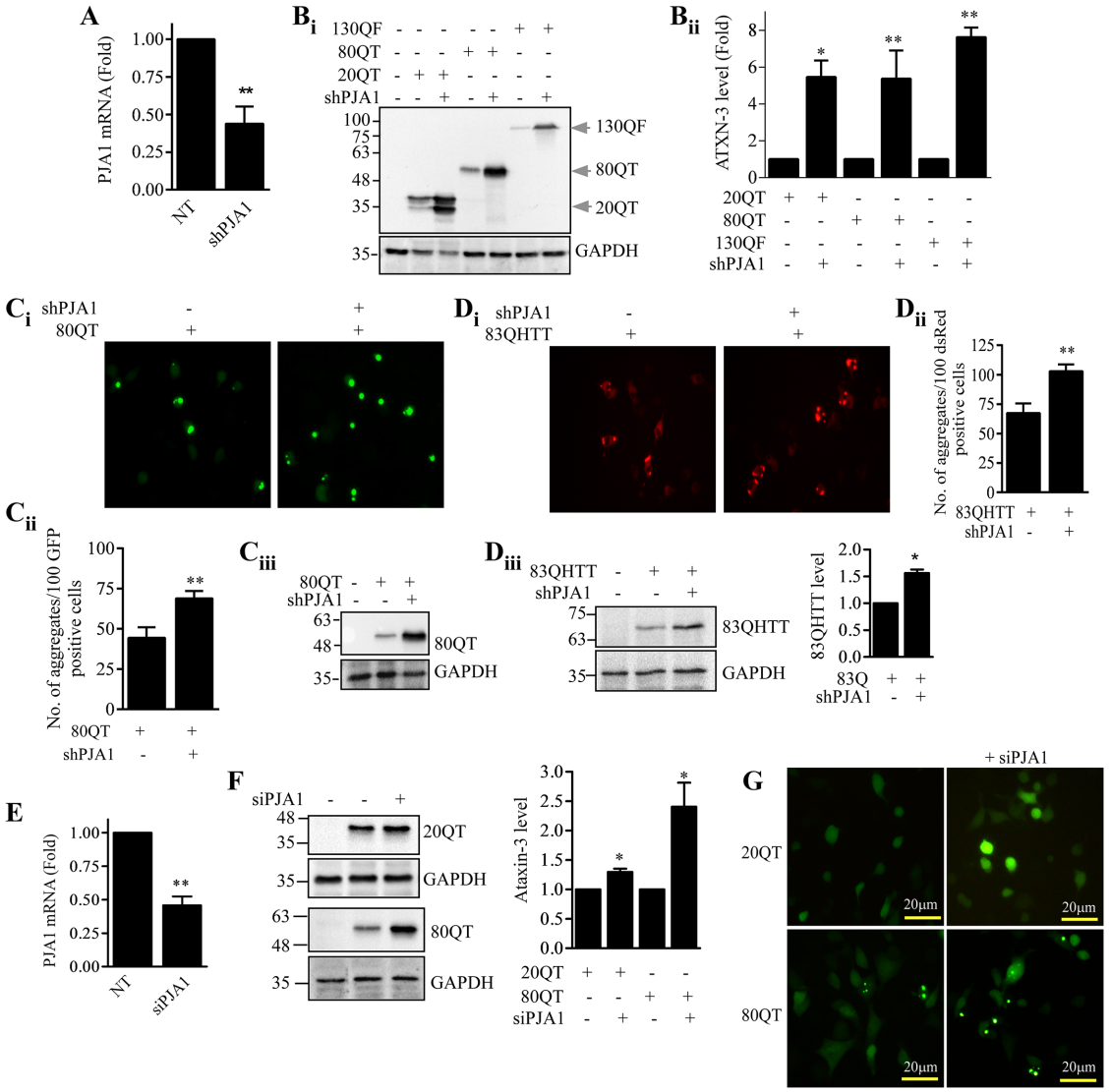

FIGURE 5: PJA1 silencing in N2A cells enhances the formation of polyQ aggregate. (A) shRNA-mediated down-regulation of PJA1 transcript level. N2A cells were transiently transfected with shRNA targeted to PJA1. Cells were harvested after 48 h. Total RNA was isolated and subjected to quantitative RT-PCR. Data were collected from three independent experiments and normalized to the levels of GAPDH. Values are the mean ± SD. Significance was calculated by *t* test. $p < 0.01$. (B) PJA1 downregulation enhances the level of ataxin-3 proteins in N2A cells. The protein levels of 20QT, 80QT, and 130QF ataxin-3 were assayed in the PJA1-silenced condition by Western blot analysis. The blots were probed with anti-GFP antibody for detection of ataxin-3. GAPDH is the loading control. The bands were quantified, normalized with GAPDH, and plotted as a bar diagram. Error bar represents SD of three independent experiments. Significance was calculated by *t* test. *, ** $p < 0.05$ and $p < 0.01$, respectively. (C, D) Down-regulation of PJA1 enhances ataxin-3 and HTT aggregates. 80QT ataxin-3 (C) or 83QHTT (D) plasmids were transfected in N2A cells upon silencing of PJA1 with shRNA. After 48 h, cells were viewed under fluorescence microscope. The aggregates were counted and plotted in a bar graph. Values are the mean ± SD. Significance was calculated by *t* test, $p < 0.01$. The same cells were processed for immunoblotting, and the blots were probed with anti-GFP, anti-DsRed, and anti-GAPDH antibodies. The 83QHTT bands were similarly quantified and plotted as bar diagram, the error bar representing SD of three independent experiments. Significance was calculated by *t* test. $p < 0.05$. (E) siRNA-mediated down-regulation of PJA1 transcript level. N2A cells were transiently transfected with scramble or siRNA targeted to PJA1. Cells were harvested after 48 h. Total RNA was isolated and subjected to quantitative RT-PCR. Data were collected from three independent experiments and normalized to the levels of GAPDH. Values are the mean ± SD. Significance was calculated by *t* test. $p < 0.01$. (F) siRNA-mediated down-regulation of PJA1 enhances the ataxin-3 protein level in N2A cells. The protein levels of 20QT and 80QT ataxin-3 were assayed in the PJA1-silenced condition by Western blot analysis. The blots were probed with anti-GFP antibody for detection of ataxin-3. GAPDH is the loading control. The bands were quantified and normalized with GAPDH and plotted as a bar diagram. Error bars represent a cumulation of three experiments performed independently. Significance was calculated by *t* test. $p < 0.05$. (G) The same cells were viewed under a fluorescence microscope, where enhanced overall fluorescence and aggregation in the PJA1-silenced condition were observed for 20QT and 80QT ataxin-3, respectively.

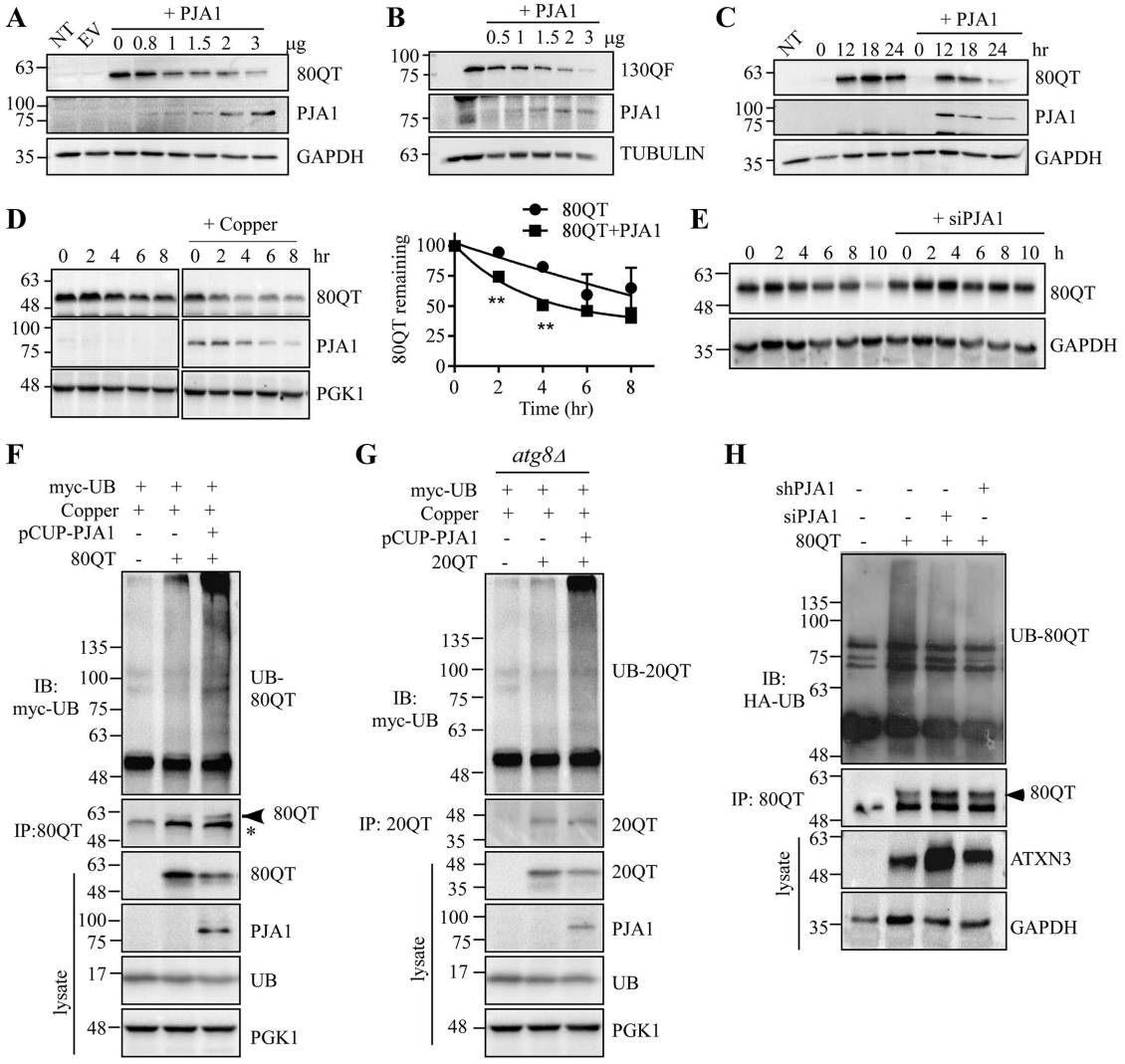

FIGURE 6: PJA1 promotes the degradation of ataxin-3 by promoting its ubiquitination. (A–C) Time- and dose-dependent expression of PJA1 enhances the degradation of ataxin-3 protein. N2A cells were transiently transfected with 80QT (A) and 130QF (B) with various concentrations of PJA1 as indicated. Twenty-four hours after transfection, the ataxin-3 level was detected in cell lysates by Western blotting with anti-GFP antibody. (C) 80QT ataxin-3 and PJA1 (3 µg) were cotransfected in N2A cells, and the cells were collected at various times as indicated. Western blot analysis shows the ataxin-3 level. GAPDH and tubulin were used as loading controls. (D, E) PJA1 facilitates the degradation of 80QT ataxin-3 in mammalian and yeast systems. (D) GAL-shutoff chase was performed to measure the turnover of ataxin-3. PJA1 expression was carried out with the addition of copper followed by induction of ataxin-3 with 2% galactose for 2 h. The expression of ataxin-3 was shut off using 2% glucose and chased for the indicated times. The ataxin-3 level was detected by Western blotting with anti-GFP antibody. PGK1 is loading control. Data were collected from three separate experiments and normalized to the levels of PGK1. The band intensities were quantified using ImageJ software and plotted in the adjacent graph. Error bar indicates SD. (E) Cycloheximide chase of 80QT ataxin-3 was done upon silencing of PJA1 with smartpool siRNA (Dharmacon) targeted to PJA1 in N2A cells as described in *Materials and Methods*. Cycloheximide (10 µg/ml) was used to stop translation and chased for 10 h. The ataxin-3 level was detected by Western blotting with anti-GFP antibody. GAPDH acts as the loading control. (F–H) PJA1 promotes the ubiquitination of ataxin-3. (F, G) 80QT and 20QT ataxin-3 plasmids were transformed along with PJA1 and myc-ubiquitin into WT (F) and *atg8*Δ (G) yeast cells, respectively. Expression of PJA1 was induced with 300 µM copper for 2 h before ataxin-3 induction with 2% galactose for 4 h. Yeast cells were then harvested, and immunoprecipitation was performed using anti-GFP antibody. The blots were probed with anti-myc and anti-GFP antibody for detection of ubiquitinated ataxin-3 and the amount of immunoprecipitated ataxin-3 respectively. Lysate shows the expression of the proteins. PGK1 was the loading control. (H) Silencing of PJA1 reduces ubiquitination of 80QT ataxin-3. PJA1 was silenced in N2A cells with either shRNA or siRNA targeted to PJA1. GFP-80QT ataxin-3 and HA-ubiquitin plasmids were cotransfected, and the ubiquitination of 80QT ataxin-3 was detected upon immunoprecipitating ataxin-3 with anti-GFP antibody followed by Western blotting with anti-HA antibody. Lysates show the expression of respective proteins. GAPDH is the loading control. *, heavy chain.

PJA1 suppresses polyQ toxicity in yeast and *Drosophila* model of SCA3

Accumulation of expanded polyQ proteins causes neuronal vulnerability, although the principal reason for its toxicity is currently unknown (Paulson *et al*., 2017). Evidence suggests polyQ expansion–driven acceleration of neuronal aging with altered nuclear integrity and nucleocytoplasmic transport in HD (Gasset-Rosa *et al*., 2017). Because PJA1 promoted degradation of ataxin-3 protein (Figures 5 and 6), it might lead to decreased proteotoxicity associated with accumulation of mutant ataxin-3. To test this, we have initially chosen yeast as a model to study polyQ-mediated toxicity. Expression of 80QT ataxin-3 from a galactose-inducible promoter in yeast causes growth retardation of yeast cells as evident from a spot assay. However, expression of PJA1 in these cells rescues yeast toxicity suggesting suppression of polyQ pathogenesis by PJA1 (Figure 8A). We further validated this result in a *Drosophila* model of SCA3. The transgenic models used in this study take advantage of the GAL4-UAS system, in which cDNAs encoding human mutant ataxin-3 (truncated 78Q; Bloomington ID-8150) are under the control of the heterologous yeast upstream activating sequence (UAS) promoter element that responds to driver lines expressing the GAL4 transcription factor. 78QT ataxin-3 under the GMR-GAL4 system shows a severe degenerative external eye phenotype; however, the GMR-GAL4-PJA1 transgenic fly was embryonically lethal. Thus, the Rhodopsin1-GAL4 (Rh1) line that is expressed following photoreceptor maturation and is active only after completion of eye development beginning in late pupal stages was selected. The transgenic PJA1 fly was stable under the GAL4-Rh1 system, and PJA1 expression levels under GAL4-Rh1 were checked (Supplemental Figure S4). Cryosectioning of transgenic *Drosophila* eyes followed by hematoxylin/eosin staining was performed. In young Rh1-78QT (8–10 d) or Rh1-PJA1, retinal sections did not exhibit specific defects in ataxin-3- or PJA1-expressing flies respectively (Figure 8B). However, in older Rh1-78QT flies (35–40 d), the retinas exhibited striking degenerative phenotypes with disorganized ommatidia and tissue dissociation associated with the appearance of vacuoles as mentioned in previous studies (Sowa *et al*., 2018). The Rh1-78QT flies with overexpressed PJA1 had, however, far less vacuole formation when compared with the Rh1-78QT, establishing PJA1's role in mitigating toxicity caused by polyQ-expanded ataxin-3 (Figure 8C). We additionally performed immunofluorescence studies of these retinal cryosections to confirm the expression of ataxin-3 and PJA1. We obtained similar morphological differences, as observed in Figure 8C. Furthermore, the aggregates formed in the case of Rh1-78QT flies were considerably fewer in flies overexpressing PJA1, which reconfirms PJA1's role in the degradation of polyQ proteins (Figure 8D, iii–v).

DISCUSSION

Eukaryotic cells are equipped with PQC machinery that eliminates damaged or misfolded proteins and relieves cells from proteotoxic stress (McKinnon and Tabrizi, 2014). However, when misfolded proteins overwhelm the capacity of the clearance machinery, they accumulate as intracellular aggregates that are toxic for the cell. PolyQ repeat proteins undertake abnormal conformation when the polyQ tract exceeds the threshold level and form intracellular inclusions/aggregates, which account for cellular toxicity, characterized by microtubule destabilization, cytoskeleton collapse, transcriptional dysfunction, and finally cell death (Trushina *et al*., 2003). The components of the PQC, the molecular chaperones, try to refold them, but on failure, shuttle them to E3 ubiquitin ligases to be tagged by ubiquitin and eventually degraded by the ubiquitin proteasome pathway or autophagy. There are several E3 ligases, viz., CHIP, Parkin, Gp78, E6-AP, MGRN1, ITCH, and Malin, that aid in the clearance of polyQ proteins and their aggregates, hence mitigating cytotoxicity (Tsai *et al*., 2003; Jana *et al*., 2005; Garyali *et al*., 2009; Ying *et al*., 2009; Chhangani and Mishra, 2013; Mishra *et al*., 2013; Chhangani *et al*., 2014). In the present study, we described the function of PJA1, a RING-H2 ubiquitin ligase highly expressed in the brain, in the degradation of polyQ proteins. PJA1 associates with polyQ proteins and leads to reduction of polyQ aggregates and cytotoxicity in cellular and *Drosophila* models of SCA3.

Proteostasis collapse or proteostatis network (PN) disruptions are fundamental in several age-onset neurodegenerative disorders (Hipp *et al*., 2014). However, the reason behind this collapse, and how it contributes to disease onset or progression, is still elusive. One hypothesis is that chronic expression of aggregation-prone polyQ-expanded proteins, α-synuclein or Aβ leads to proteasomal and autophagy impairment, which drive the cellular disruptions observed in most neurodegenerative disorders such as HD, PD, and AD (Gregori *et al*., 1995; Keller *et al*., 2000; McNaught and Jenner, 2001; Komatsu *et al*., 2006; Winslow *et al*., 2010; Hipp *et al*., 2012). Our observation strengthens the hypothesis. We found reduced levels of PJA1 transcript and protein in cells expressing polyQ proteins. The simple explanation could be the fact that polyQ aggregates sequester transcription factors such as nuclear factor kappa-light-chain-enhancer of activated B cells (NF-κB), CREB-binding protein (CBP), and TATA box–binding protein (TBP), which as a consequence lose their normal cellular functions (Shimohata *et al*., 2000; Dunah *et al*., 2002; Schaffar *et al*., 2004; Goswami *et al*., 2006). The aberrant function of transcription factors thus contributes to enhanced pathogenesis of polyQ diseases. These findings also led us to speculate on the interaction of PJA1 with polyQ proteins as polyQ aggregates sequester components of the PQC, ubiquitin ligases such as MGRN1, CHIP, and Malin, and hence the unavailability of a functioning cellular surveillance system may also be responsible for disease pathogenicity. Likewise, we find PJA1 interaction with wild-type as well as mutant ataxin-3/huntingtin proteins and also their aggregates (Figures 2 and 3). A recent report establishing PJA1's role in reducing TDP43 aggregate formation and pathogenesis associated with amyotrophic lateral sclerosis (ALS) and frontotemporal lobar degeneration (FTLD) also supported our hypothesis (Watabe *et al*., 2020).

These results impelled us to identify PJA1's functional role in the proteostasis of polyQ proteins. Our observations established a marked decrease in the number of polyQ aggregates by PJA1, which was not detected in the case of the RING domain–deleted PJA1 (Figure 4). The finding was confirmed by shRNA/siRNA-mediated knockdown of PJA1, which resulted in an increase in the polyQ aggregate count and their protein levels (Figures 5 and 6G). This led us to postulate PJA1's role as an E3 ubiquitin ligase in the degradation of ataxin-3 and hence the removal of aggregates. Previously, PJA1's role had been established in the degradation of proteins such as MAGE-D1/Dlxin-1 and EZH2 involved in osteoblast differentiation and myogenesis, respectively (Sasaki *et al*., 2002; Consalvi *et al*., 2017). Overexpression of PJA1 has been found in cancers such as glioblastomas and gastrointestinal cancer where the adaptor protein ELF of tumor suppressor SMAD3 is degraded (Saha *et al*., 2006; Chen *et al*., 2020). But the function of PJA1 in the degradation of polyQ proteins had not been studied previously. Ubiquitin ligases work by tagging ubiquitin to substrates for their recognition by the proteosomal machinery/autophagy for their degradation (Deshaies and Joazeiro, 2009). In line with that, we found enhanced ubiquitination of ataxin-3 in the presence of PJA1 but diminished ubiquitinated ataxin-3 when PJA1 was silenced, indicating PJA1's ability

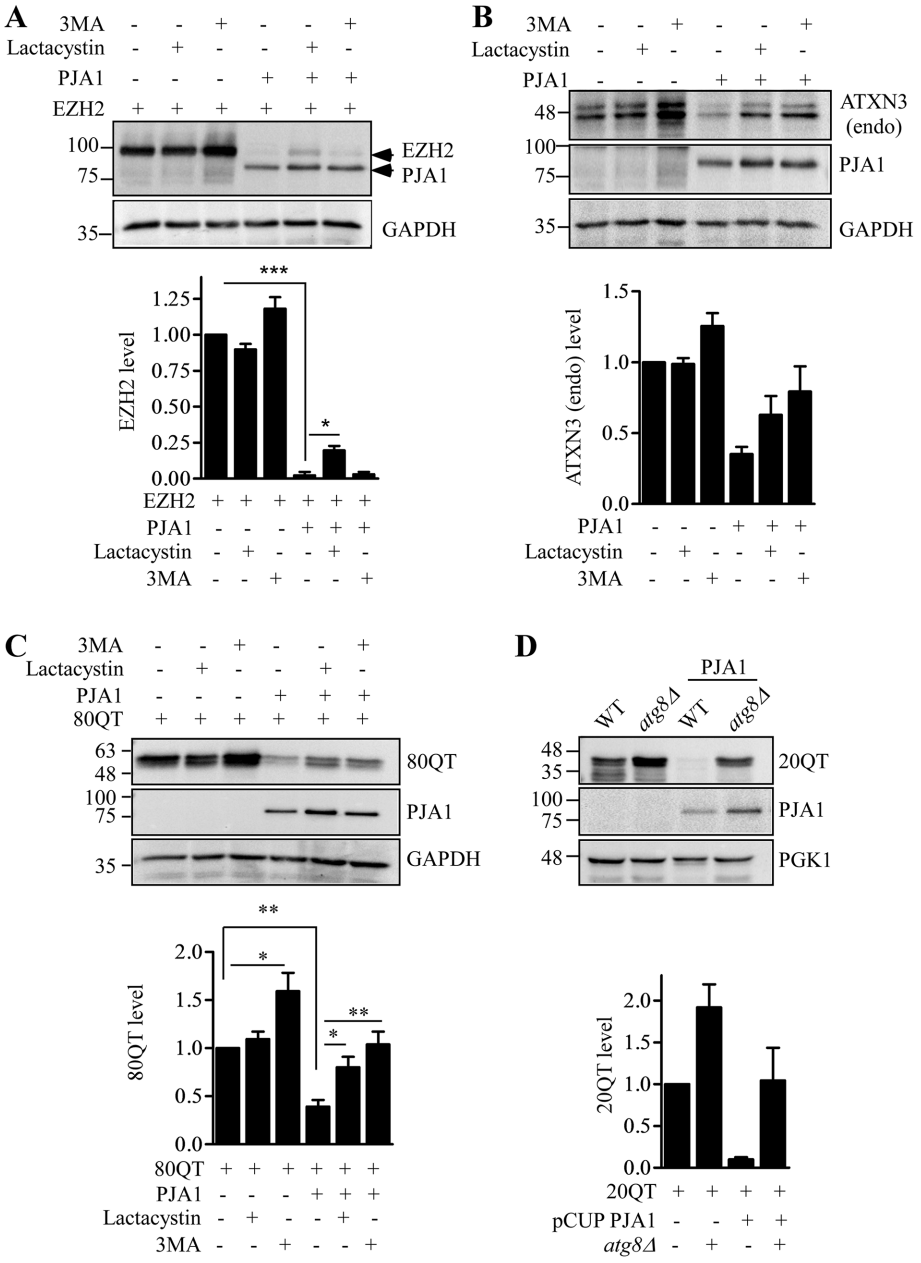

FIGURE 7: PJA1 facilitates the degradation of ataxin-3 through proteasome and autophagy. (A) PJA1-mediated proteasomal degradation of EZH2 protein. EZH2 and PJA1 were cotransfected in HEK293T cells. Cells were treated with either proteasomal inhibitor lactacystin (2 μM) or lysosomal inhibitor 3MA (4 nM) for 6 h before harvesting the cells. EZH2 and PJA1 levels were detected by Western blotting with anti-HA antibody. GAPDH is loading control. Data collected from three separate experiments were normalized to the levels of GAPDH. The band intensities were quantified using ImageJ software and plotted in the graph. Error bar indicates SD. Significance was calculated by *t* test. * $p < 0.05$, *** $p < 0.001$. (B–D) PJA1 clears ataxin-3 via proteasome and autophagy. (B) The endogenous ataxin-3 level was monitored upon overexpression of PJA1 in HEK293T cells treated with lactacystin or 3MA. The graph was plotted using data from two different experiments. (C) 80QT ataxin-3 and PJA1 were coexpressed in HEK293T. The ataxin-3 level was assayed by Western blot analysis upon treating the cells with lactacystin or 3MA. The bands were quantified and normalized with GAPDH and plotted in the graph. Values are the mean ± SD. Significance was calculated by *t* test. * $p < 0.05$, ** $p < 0.01$. (D) Knockout of *ATG8* rescued PJA1-mediated degradation of 20QT ataxin-3 in yeast. p315GAL-GFP-20QT ataxin-3 and p426CUP-HA-PJA1 plasmids were transformed into *atg8*Δ yeast strains. PJA1 expression was induced with 300 μM copper followed by ataxin-3 with 2% galactose. Overexpressed and endogenous ataxin-3 levels were monitored by Western blotting using anti-GFP and anti–SCA3-1H9 antibodies, respectively. Data from two separate experiments were plotted as bar diagrams. GAPDH (panels A–C) and PGK1 (panel D) were used as loading controls.

to ubiquitinate polyQ proteins (Figure 6). Notably, PJA1-mediated degradation of polyQ proteins occurs via the proteasome as well as lysosomal pathway, although further study is needed to establish the preferential pathway or dependency on substrates.

Clearance of misfolded proteins from cells leads to reduction in their accumulation and associated cellular toxicity. Our results thus prompted us to examine the consequential effects of removal of aggregates and degradation of polyQ proteins by PJA1. Previously CHIP, UBR5, and UBE3A have been shown to mitigate polyQ-induced toxicity in cellular as well as animal models of polyQ diseases (Miller *et al.*, 2005; Maheshwari *et al.*, 2014; Koyuncu *et al.*, 2018). Similar to these ubiquitin ligases, PJA1 is capable of reducing the growth sensitivity of yeast associated with polyQ protein and rescuing the retinal degeneration in the *Drosophila* model of SCA3 (Figure 8). This result suggests a cytoprotective response of PJA1 against polyQ-induced toxicity in yeast as well as *Drosophila*.

Interestingly, studies spanning all polyQ disorders hypothesize the presence of a tissue-specific proteostasis network (PN). PN heterogeneity encompasses all classes of chaperone, autophagy mediators, UPS components, and stress response regulators and these molecules exibit profoundly altered expression patterns between tissues (Powers *et al.*, 2009; Tebbenkamp and Borchelt, 2010; Guisbert *et al.*, 2013). Previous studies have also hinted at how PN heterogeneity can influence disease presentation and progression (Tagawa *et al.*, 2007; Tsvetkov *et al.*, 2013). Hence deciphering the entire complex PN in polyQ disorders might help us understand the major chaperones and degradative components at work. And, because the requirements of the PQC by the substrates vary based on tissue type, there might be a robust PN working in the brain that modulates normal or neurodegenerative disease–related proteins. PJA1 serves as a crucial E3 ligase of the brain proteome that is recruited to TDP43 (Watabe *et al.*, 2020) and polyQ proteins like ataxin-3 and huntingtin for their degradation and hinders their aggregation; thus dysfunction of this E3 ligase might result in pathogenesis and onset of neurodegeneration. In conclusion, our results suggest that modulation of PJA1 might serve as potential therapy for polyQ disorders and result in weakened pathogenesis of the diseases.

MATERIALS AND METHODS

Request a protocol through *Bio-protocol*.

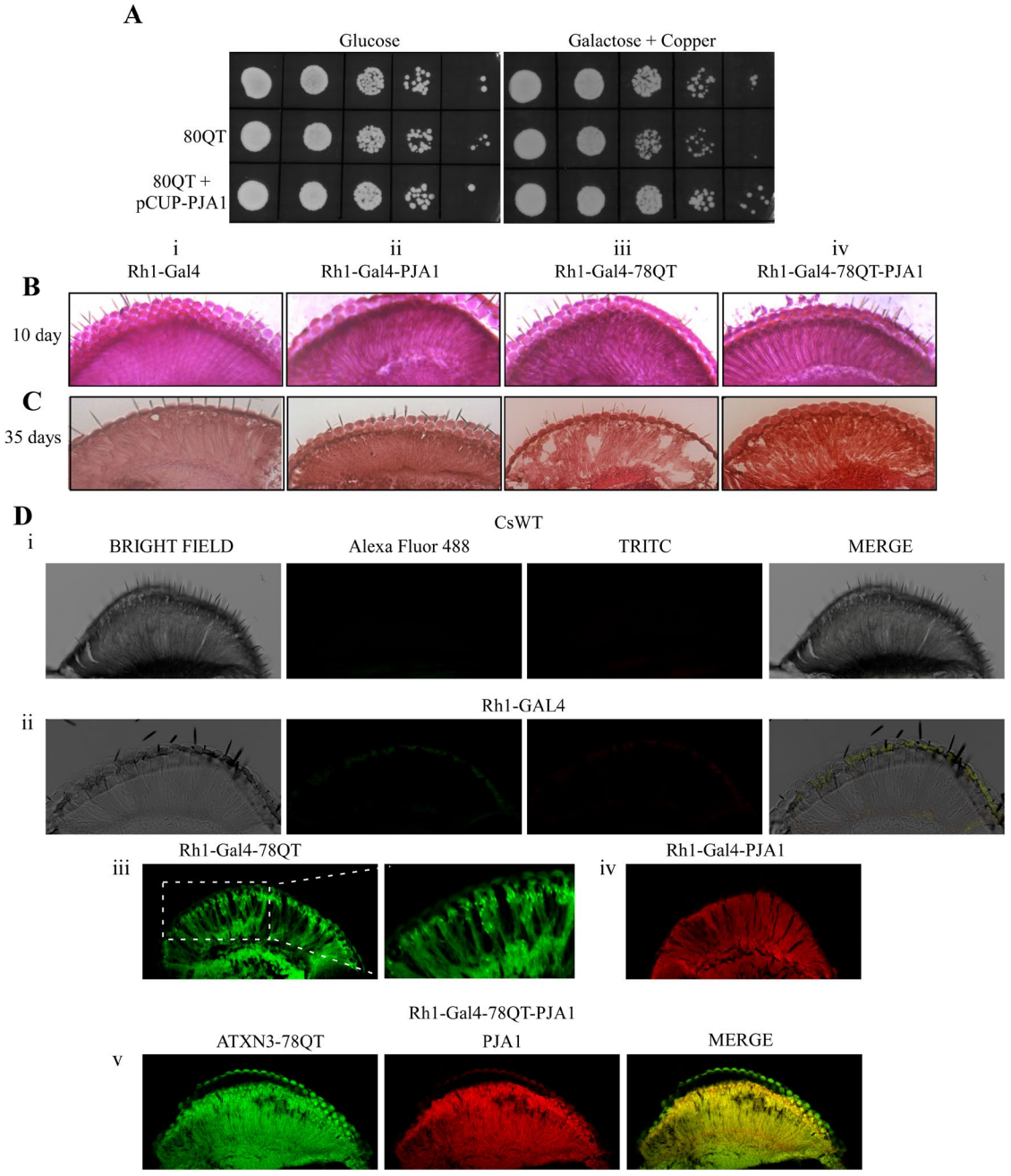

FIGURE 8: PJA1 suppresses polyQ toxicity in yeast and the *Drosophila* model of SCA3. (A) PJA1 suppresses polyQ-mediated toxicity in yeast. Yeast cells harboring p315GAL-80QT ataxin-3 and p426CUP-PJA1 were grown overnight in 2% raffinose. PJA1 was induced with 300 µM copper for 2 h, followed by induction of ataxin-3 with 2% galactose. The cultures were serially diluted and spotted onto either Yeast extract Peptone Dextrose (YPD) or YP with 2% galactose and 100 µM copper. The plates were incubated at 30°C. Growth of yeast cells were observed after 48 h. (B, C) PJA1 rescues polyQ-induced toxicity in the *Drosophila* eye. (Bi–iv) Retinal sections of the *Drosophila* eye of 8–10-d-old fly. Retinal sections of mutant ataxin-3 expressing transgenic *Drosophila* eye showed identical phenotype with the control fly. Notably, *Drosophila*-expressing PJA1 did not exhibit any change in retinal morphology. (C) Thirty-five- to forty-day-old fly developed retinal vacuole formation and photoreceptor disorganization induced by mutant ataxin-3 (iii). Overexpression of PJA1 in mutant ataxin-3–expressing *Drosophila* results in retinal sections with fewer vacuoles and an overall rescue of phenotype. ($n = 10$ per genotype). (D) Immunofluorescence of the retinal cryosections of the 35–40-d-old flies expressing mutant ataxin-3 (iii), PJA1 (iv) alone, and coexpression of mutant ataxin-3 and PJA1 (v). The CsWT (i) and Rh1-GAL4 (ii) flies were taken as control. Alexa Fluor 488 and TRITC secondary antibodies were used to immunostain HA-tagged 78QT ataxin-3 and PJA1, respectively.

Strains, reagents, and antibodies

Yeast strain BY4741 (MATa his3Δ0 leu2Δ0 met15Δ0 ura3Δ0) was used in this study. Autophagy-impaired *atg8::Kanmx* was obtained from a yeast knockout library. Lactacystin and 3-methyladenine (3MA) were purchased from Sigma. The following primary antibodies were used: mouse monoclonal antibodies against SCA3-1H9,

DsRed (Merck-Millipore), FLAG, HA (Sigma), GFP (Roche), Ub (Cell Signaling Technology), PGK1 (Invitrogen); rabbit monoclonal antibodies against α-tubulin, GAPDH (BioBharati LifeScience, India), MYC, GFP (Cell Signaling Technology), PJA1 (Genetex). The secondary antibodies, goat anti-mouse immunoglobulin G–horseradish peroxidase (IgG-HRP) antibody and anti-rabbit IgG-HRP were obtained from Jackson Laboratory.

Plasmid constructs

Ataxin-3 constructs (pEGFP-N1-20QT, pEGFP-N1-20QF, pEGFP-N1-80QT, and pEGFP-N1-130QF) were kindly provided by Nihar Ranjan Jana (Indian Institute of Technology, Kharagpur, India). Mouse PJA1 in vectors pCMV-HA-PJA1 and pEGFP-C1-PJA1 were a gift from Oliver Stork (Otto-von-Guericke University Magdeburg, Germany). Exon1 of pEGFP-C1-16Q and pDsRed-C1-83Q huntingtin were also obtained from Debashis Mukhopadhyay (Saha Institute of Nuclear Physics, India). The yeast constructs p315GAL-20QT-GFP and p315GAL-80QT-GFP were generated by standard PCR methods. 20QT and 80QT were first amplified by PCR using primers 5′FLAG *Bam*H1-CGCGGATCCATGGACTACAAAGACGATGACGACAAGCAAGGTAGTTCCAG and 5′ *Not*1TTTTCCTTTTGCGGCCGCCTAGATCACTCC (without stop codon). The full open reading frame (ORF) (20QT/80QT) was then cloned into the p315GAL plasmid digested with *Bam*H1 and *Not*1. The ORF of GFP was digested from the YEp53 plasmid using the *Not*1 restriction enzyme and inserted after 20QT and 80QT. PJA1 was amplified from pEGFP-C1-PJA1 using primers 5′HA *Hin*dIII-CCCAAGCTTATGTACCCATACGATGTTCCAGATTACGCTAGCCACCAGGAAAGGA and 5′ *Xho*1-CCGCTCGAGTTAGAGCGGGGGAGGGAAC and cloned into the p426CUP vector. The deletion mutants and point mutations of PJA1 were obtained by using standard PCR and site-directed mutagenesis protocols. pDsRed-C1-PJA1 was generated by subcloning from pEGFP-C1-PJA1. All constructs were confirmed by sequencing. The plasmids used in this study are shown in Supplemental Table S1.

Cell culture and transfection

HEK293T, HEK293, and N2A cells were obtained from the National Centre for Cell Science (NCCS), Pune, India. The cells were cultured in DMEM (HiMedia Laboratories, India) containing 10% fetal bovine serum (FBS) (Life Technologies) in a humidified chamber with 5% CO_2. The plasmid DNA was transfected using Lipofectamine LTX with plus reagent (ThermoFisher) or PEI (polyetheleneimine; Polysciences) at 70% confluence in DMEM without serum. shRNA/siRNA transfection was carried out with Lipofectamine 2000 (ThermoFisher) according to the manufacturer's protocol.

Western blot analysis

Cells were first lysed in RIPA buffer containing 50 mM Tris-HCl (pH 7.5), 150 mM NaCl, 1 mM EDTA, 0.1% SDS, and 1 mM phenylmethylsulfonyl fluoride (PMSF) with protease inhibitor cocktail. Cell lysates were cleared at 12,000 × *g* for 20 min at 4°C. Proteins were estimated using the Bicinchoninic acid (BCA) protein estimation kit (ThermoFisher) and subsequently separated by 10% SDS–PAGE and transferred onto nitrocellulose membrane (Pall Corporation). The proteins were visualized using ECL detection buffer, and the image was captured in the Chemidoc MP system (BioRad). Image analysis was done by ImageJ software. Statistical analysis was scored using GraphPad Prism software.

Immunoprecipitation

Cells were lysed in buffer containing 50 mM Tris, pH 7.5, 150 mM NaCl, 0.1% NP-40, 1 mM PMSF, and protease inhibitor cocktail. Cellular debris was removed by centrifugation at 12,000 × *g* for 15 min at 4°C. Protein concentration was estimated by the BCA method. The cell lysates were incubated with antibody in immunoprecipitation (IP) dilution buffer (50 mM Tris, pH 7.5, 150 mM NaCl, 0.1% NP-40, PMSF) overnight at 4°C with gentle rotation. The next day, a protein A–Sepharose (GE Healthcare) bead preequilibrated with IP dilution buffer was added and nutated further for 2 h at 4°C for immunoprecipitation. The beads were then washed three times with IP dilution buffer. Bound proteins were eluted from beads with SDS sample buffer, vortexed, boiled for 5 min, and analyzed by Western blotting.

Microscopic analysis

HEK293T cells were transfected with polyQ proteins ataxin-3 (pEGFP-N1-80QT and 130QF) or huntingtin (16Q and 83Q) alone and with pCMV-HA-PJA1. Twenty-four hours after transfection, cells were viewed under a fluorescence microscope at 20× (Leica). Aggregates were counted per 100 GFP-positive cells from 10 randomly chosen fields.

For confocal imaging, HEK293T cells were grown on cover slips coated with 0.01% poly-L-lysine. DNA transfection was carried out at 60% confluence. After 24 h the cells were fixed with 3.7% formaldehyde, washed with phosphate-buffered saline (PBS) for 5 min, and mounted on glass slides with Distyrene, a Plasticizer, and Xylene (DPX). The slides were let dry at room temperature and sealed with nail polish. Cells were visualized at 63× oil objective in a Leica TCS SP8 confocal microscope.

Degradation assay

Yeast cells were transformed with p315GAL-80QT ataxin-3 and p426CUP-PJA1 plasmids, and the tranformants were selected with synthetic dropout media without leucine and uracil (SD-Leu-Ura). The transformed cells were grown overnight in synthetic dropout media with 2% raffinose. PJA1 expression was promoted by the addition of 300 μM copper. After 2 h of PJA1 expression, 2% galactose was added for induction of ataxin-3 protein. Ataxin-3 induction was blocked after 2 h by the addition of 2% glucose and then chased further for 8 h. Cells were harvested at regular time intervals.

For cycloheximide chase analysis of 80QT ataxin-3 in the PJA1-silenced condition, N2A cells were transfected with scrambled and smartpool siRNA specific for PJA1. Six hours later, the cells were seeded freshly. Eighteen hours after siRNA transfection, cells were transfected with pEGFP-N1-80QT ataxin-3. Cycloheximide (10 μg/ml) was added to the cells to impede translation and chased further for 10 h with harvesting the cells at regular time intervals.

Spot assay

Yeast cells transformed with p315GAL-80QT-ataxin-3 and p426CUP-PJA1 plasmids were grown overnight in synthetic dropout media without leucine and uracil containing 2% raffinose. Copper (300 μM) was added to induce PJA1 for 2 h, followed by the addition of 2% galactose for induction of ataxin-3. Cells were grown until OD_{600} 0.5. The cultures were diluted serially and spotted onto a Yeast extract and Peptone (YP) plate in the presence of either 2% galactose with 100 μM copper or 2% glucose media. The plates were kept at 30°C for 2 d.

Ubiquitination assay

N2A cells were transfected with PJA1-specific siRNA and shRNA. Six hours after transfection, the cells were seeded freshly for the next set of transfection. Eighteen hours after siRNA transfection, the cells were transfected with pCMV-HA-ubiquitin and pEGFP-N1-80QT. Autophagy inhibitor 3-MA or proteasome inhibitor lactacystin was

added to the cells 6 h before harvesting the cells. The cells were then lysed with cell lysis buffer (10 mM Tris-HCl, pH 8.0, 150 mM NaCl, 2% SDS, 1 mM PMSF with protease inhibitor cocktail). Protein was estimated by the BCA method. The lysates were diluted 10 times with IP dilution buffer (10 mM Tris-HCl, pH 8.0, 150 mM NaCl, 2 mM EDTA, 1% Triton); anti-GFP antibody was added to the lysate. and the immunocomplex was incubated at 4°C overnight with gentle shaking. The next day, protein A–Sepharose (GE Healthcare) beads were added to the cell lysate–antibody mixture and incubated at 4°C for 2 h. The resin was then washed three times with wash buffer (10 mM Tris-HCl, pH 8.0, 1 M NaCl, 1 mM EDTA, 1% NP-40) and boiled with 2×SDS loading buffer for immunoblot analysis.

Reverse transcriptase PCR analysis and semiquantitative RT-PCR analysis

N2A cells were transfected with normal and expanded polyQ protein. After 72 h of transfection cells were harvested, and total RNA was isolated with TRIzol reagent (Qiagen). cDNA was synthesized by using a RT-PCR kit (Life Technologies). The RT-PCR was performed by using SYBR green super mix (Applied Biosystems) using an iCycler iQ RT Thermocycler Detection System (Applied Biosystems). The RT-PCR analysis conditions were the same for both PJA1 and GAPDH. The following primers were used for detection of PJA1: forward 5′-GCAATGGCAGTGGTTATCCT-3′ and reverse 5′-ACATCCCAGGCTGTATGAGC-3′; (GAPDH was used as control.) forward 5′-ACCCAGAAGACTGTGGATGG-3′ and reverse 5′-CACATTGGGGGTAGGAACAC-3′. All reactions were carried out in triplicate with negative controls lacking the template DNA.

RNA interference

Smartpool siRNA of mouse PJA1 was purchased from Dharmacon. shRNA targeted to mouse PJA1 was generated using the pLKO.1 shRNA protocol. The primers used for generating shRNA of PJA1 are forward 5′-CCGGCACCGACGATTACTACCGATACTCTCGAGAGTATCGGTAGTAATCGTCGGTGTTTTTG and reverse 5′-AATTCAAAAACACCGACGATTACTACCGATACTCTCGAGAGTATCGGTAGTAATCGTCGGTG.pEGFP-N1-20QT/80QT/130QFATXN3–and pDsRed-C1-83Q HTT–expressing cells were transiently transfected with siRNA, shRNA of PJA1, and control siRNA according to the manufacturer's protocol.

Drosophila stocks and husbandry

Fly stocks and crosses were maintained at standard condition (25°C). Rh1-GAL4 was employed for overexpressing various transgenes (Xiong *et al.*, 2012). An UAST-PJA1 transgenic fly was generated. PJA1 was digested from the pCMV-HA-PJA1 construct using *Not*1- and *Kpn*1-specific forward and reverse primers, respectively, and cloned into the pUAST plasmid vector (Brand and Perrimon, 1993). The plasmid clones were sent to Centre for Cellular and Molecular Platforms (CCAMP), Bangalore, subcloned into pUAST-attB, and then used for microinjection and targeted integration into the third chromosome. Transgenic flies were scored based on eye color marker, and the stocks were subsequently balanced. Rh1-GAL4 was used to drive the transgene, and the expression of PJA1 was confirmed by Western blot analysis. UAS-Hsap\MJD.tr-Q78 flies harboring the previously reported truncated ataxin-3 construct were obtained from the Bloomington Stock Centre (#8150). Genetic crosses were carried out to make stable stocks by combining this construct with UAST-PJA1 and UAS dicer2 (Bloomington #24644), respectively. Experiments were carried out by crossing Rh1 GAL4 flies to the respective genotypes. The progeny flies were sorted for the appropriate genotypes and were maintained at 25°C by regular transfer to a new vial of fly food. Retinal histology was carried out on 8–10- and 35–40-d-old flies.

Retinal histology

Adult fly heads were fixed in 3.7% formaldehyde for 60–90 min in ice. They were next treated with a gradient of sucrose solutions and subsequently placed in 30% sucrose overnight. The next day 5-µm frontal retinal sections were obtained using microtome (Leica). The sections were postfixed with 3.7% formaldehyde and stained with hematoxylin and eosin and observed under the microscope at 20× (Leica). At least 10 animals were examined for each genotype.

Immunofluorescence of retinal sections

The retinal cryosections were fixed in 0.5% formaldehyde in 1× PBS for 30 min, followed by thorough rinses in 1× PBS. The slides were washed in 0.05% Triton X-100 and then blocked in 3% Bovine serum albumin for 1 h. The slides were next incubated in the corresponding primary antibodies overnight. The next day, the slides were washed and again incubated in goat-anti-rabbit and goat-anti-mouse antibodies conjugated to TRITC and Alexa Fluor 488, respectively for 1 h. This was followed by PBS washes, air-drying the slides, and mounting with DPX mountant. The slides were viewed at 20× under a confocal microscope.

ACKNOWLEDGMENTS

We thank Nitai P. Bhattacharya for his generous amount of input for this study. We are thankful to Oliver Stork, Debashis Mukhopadhyay, and Nihar R. Jana for gifting the PJA1, huntingtin, and ataxin-3 constructs, respectively. We thank the Bloomington Drosophila Stock Center for various *Drosophila* stocks and CCAMP Bangalore, India, for generating the UAST-PJA1 transgenic flies. We also thank Rakesh Mishra, V. Bharathi, Vijayishwer Singh Jamwal, and Jayashish Ghosh for their help with cryosectioning; Sahana Mitra, Joydeep Roy, Nilanjan Gayen, Soumita Mukherjee, Somesh Roy, Madhuparna Chakraborty, and Upama Chowdhury for their helpful discussions about the work. This work was supported by the Bose Institute Intramural fund.

REFERENCES

Bence NF, Sampat RM, Kopito RR (2001). Impairment of the ubiquitin-proteasome system by protein aggregation. Science 292, 1552–1555.

Bennett EJ, Bence NF, Jayakumar R, Kopito RR (2005). Global impairment of the ubiquitin-proteasome system by nuclear or cytoplasmic protein aggregates precedes inclusion body formation. Mol Cell 17, 351–365.

Brand AH, Perrimon N (1993). Targeted gene expression as a means of altering cell fates and generating dominant phenotypes. Development 118, 401–415.

Brehme M, Voisine C, Rolland T, Wachi S, Soper JH, Zhu Y, Orton K, Villella A, Garza D, Vidal M, *et al.* (2014). A chaperome subnetwork safeguards proteostasis in aging and neurodegenerative disease. Cell Rep 9, 1135–1150.

Chai Y, Koppenhafer SL, Shoesmith SJ, Perez MK, Paulson HL (1999). Evidence for proteasome involvement in polyglutamine disease: localization to nuclear inclusions in SCA3/MJD and suppression of polyglutamine aggregation in vitro. Hum Mol Genet 8, 673–682.

Chen J, Mitra A, Li S, Song S, Nguyen BN, Chen JS, Shin JH, Gough NR, Lin P, Obias V, *et al.* (2020). Targeting the E3 ubiquitin ligase PJA1 enhances tumor-suppressing TGF-beta signaling. Cancer Res 80, 1819–1832.

Chhangani D, Mishra A (2013). Mahogunin ring finger-1 (MGRN1) suppresses chaperone-associated misfolded protein aggregation and toxicity. Sci Rep 3, 1972.

Chhangani D, Upadhyay A, Amanullah A, Joshi V, Mishra A (2014). Ubiquitin ligase ITCH recruitment suppresses the aggregation and cellular toxicity of cytoplasmic misfolded proteins. Sci Rep 4, 5077.

Consalvi S, Brancaccio A, Dall'Agnese A, Puri PL, Palacios D (2017). Praja1 E3 ubiquitin ligase promotes skeletal myogenesis through degradation of EZH2 upon p38alpha activation. Nat Commun 8, 13956.

Cui L, Jeong H, Borovecki F, Parkhurst CN, Tanese N, Krainc D (2006). Transcriptional repression of PGC-1alpha by mutant huntingtin leads to mitochondrial dysfunction and neurodegeneration. Cell 127, 59–69.
Deshaies RJ, Joazeiro CA (2009). RING domain E3 ubiquitin ligases. Annu Rev Biochem 78, 399–434.
Djajadikerta A, Keshri S, Pavel M, Prestil R, Ryan L, Rubinsztein DC (2020). Autophagy induction as a therapeutic strategy for neurodegenerative diseases. J Mol Biol 432. 2799–2821.
Dunah AW, Jeong H, Griffin A, Kim YM, Standaert DG, Hersch SM, Mouradian MM, Young AB, Tanese N, Krainc D (2002). Sp1 and TAFII130 transcriptional activity disrupted in early Huntington's disease. Science 296, 2238–2243.
Durcan TM, Fon EA (2011). Mutant ataxin-3 promotes the autophagic degradation of parkin. Autophagy 7, 233–234.
Durcan TM, Fon EA (2013). Ataxin-3 and its e3 partners: implications for Machado-Joseph disease. Front Neurol 4, 46.
Durcan TM, Kontogiannea M, Thorarinsdottir T, Fallon L, Williams AJ, Djarmati A, Fantaneanu T, Paulson HL, Fon EA (2011). The Machado-Joseph disease-associated mutant form of ataxin-3 regulates parkin ubiquitination and stability. Hum Mol Genet 20, 141–154.
Gardiner SL, Trompet S, Sabayan B, Boogaard MW, Jukema JW, Slagboom PE, Roos RAC, van der Grond J, Aziz NA (2019). Repeat variations in polyglutamine disease-associated genes and cognitive function in old age. Neurobiol Aging 84, 236e217–236e236.e228.
Garyali P, Siwach P, Singh PK, Puri R, Mittal S, Sengupta S, Parihar R, Ganesh S (2009). The malin-laforin complex suppresses the cellular toxicity of misfolded proteins by promoting their degradation through the ubiquitin-proteasome system. Hum Mol Genet 18, 688–700.
Gasset-Rosa F, Chillon-Marinas C, Goginashvili A, Atwal RS, Artates JW, Tabet R, Wheeler VC, Bang AG, Cleveland DW, Lagier-Tourenne C (2017). Polyglutamine-expanded huntingtin exacerbates age-related disruption of nuclear integrity and nucleocytoplasmic transport. Neuron 94, 48–57.e44.
Goswami A, Dikshit P, Mishra A, Nukina N, Jana NR (2006). Expression of expanded polyglutamine proteins suppresses the activation of transcription factor NFkappaB. J Biol Chem 281, 37017–37024.
Gregori L, Fuchs C, Figueiredo-Pereira ME, Van Nostrand WE, Goldgaber D (1995). Amyloid beta-protein inhibits ubiquitin-dependent protein degradation in vitro. J Biol Chem 270, 19702–19708.
Guisbert E, Czyz DM, Richter K, McMullen PD, Morimoto RI (2013). Identification of a tissue-selective heat shock response regulatory network. PLoS Genet 9, e1003466.
Hipp MS, Park SH, Hartl FU (2014). Proteostasis impairment in protein-misfolding and -aggregation diseases. Trends Cell Biol 24, 506–514.
Hipp MS, Patel CN, Bersuker K, Riley BE, Kaiser SE, Shaler TA, Brandeis M, Kopito RR (2012). Indirect inhibition of 26S proteasome activity in a cellular model of Huntington's disease. J Cell Biol 196, 573–587.
Jana NR, Dikshit P, Goswami A, Kotliarova S, Murata S, Tanaka K, Nukina N (2005). Co-chaperone CHIP associates with expanded polyglutamine protein and promotes their degradation by proteasomes. J Biol Chem 280, 11635–11640.
Ke YD, Dramiga J, Schutz U, Kril JJ, Ittner LM, Schroder H, Gotz J (2012). Tau-mediated nuclear depletion and cytoplasmic accumulation of SFPQ in Alzheimer's and Pick's disease. PLoS One 7, e35678.
Keller JN, Hanni KB, Markesbery WR (2000). Impaired proteasome function in Alzheimer's disease. J Neurochem 75, 436–439.
Komatsu M, Waguri S, Chiba T, Murata S, Iwata J, Tanida I, Ueno T, Koike M, Uchiyama Y, Kominami E, Tanaka K (2006). Loss of autophagy in the central nervous system causes neurodegeneration in mice. Nature 441, 880–884.
Koyuncu S, Saez I, Lee HJ, Gutierrez-Garcia R, Pokrzywa W, Fatima A, Hoppe T, Vilchez D (2018). The ubiquitin ligase UBR5 suppresses proteostasis collapse in pluripotent stem cells from Huntington's disease patients. Nat Commun 9, 2886.
Kuang E, Qi J, Ronai Z (2013). Emerging roles of E3 ubiquitin ligases in autophagy. Trends Biochem Sci 38, 453–460.
Maheshwari M, Shekhar S, Singh BK, Jamal I, Vatsa N, Kumar V, Sharma A, Jana NR (2014). Deficiency of Ube3a in Huntington's disease mice brain increases aggregate load and accelerates disease pathology. Hum Mol Genet 23, 6235–6245.
McKinnon C, Tabrizi SJ (2014). The ubiquitin-proteasome system in neurodegeneration. Antioxid Redox Signal 21, 2302–2321.
McNaught KS, Jenner P (2001). Proteasomal function is impaired in substantia nigra in Parkinson's disease. Neurosci Lett 297, 191–194.
Miller-Fleming L, Giorgini F, Outeiro TF (2008). Yeast as a model for studying human neurodegenerative disorders. Biotechnol J 3, 325–338.
Miller VM, Nelson RF, Gouvion CM, Williams A, Rodriguez-Lebron E, Harper SQ, Davidson BL, Rebagliati MR, Paulson HL (2005). CHIP suppresses polyglutamine aggregation and toxicity in vitro and in vivo. J Neurosci 25, 9152–9161.
Mishra A, Maheshwari M, Chhangani D, Fujimori-Tonou N, Endo F, Joshi AP, Jana NR, Yamanaka K (2013). E6-AP association promotes SOD1 aggresomes degradation and suppresses toxicity. Neurobiol Aging 34, 1310.e11–23.
Mishra L, Tully RE, Monga SP, Yu P, Cai T, Makalowski W, Mezey E, Pavan WJ, Mishra B (1997). Praja1, a novel gene encoding a RING-H2 motif in mouse development. Oncogene 15, 2361–2368.
Nixon RA (2013). The role of autophagy in neurodegenerative disease. Nat Med 19, 983–997.
Paulson H (2012). Machado-Joseph disease/spinocerebellar ataxia type 3. Handb Clin Neurol 103, 437–449.
Paulson HL, Shakkottai VG, Clark HB, Orr HT (2017). Polyglutamine spinocerebellar ataxias—from genes to potential treatments. Nat Rev Neurosci 18, 613–626.
Powers ET, Morimoto RI, Dillin A, Kelly JW, Balch WE (2009). Biological and chemical approaches to diseases of proteostasis deficiency. Annu Rev Biochem 78, 959–991.
Ryan MM, Lockstone HE, Huffaker SJ, Wayland MT, Webster MJ, Bahn S (2006). Gene expression analysis of bipolar disorder reveals down-regulation of the ubiquitin cycle and alterations in synaptic genes. Mol Psychiatry 11, 965–978.
Saha T, Vardhini D, Tang Y, Katuri V, Jogunoori W, Volpe EA, Haines D, Sidawy A, Zhou X, Gallicano I, *et al.* (2006). RING finger-dependent ubiquitination by PRAJA is dependent on TGF-beta and potentially defines the functional status of the tumor suppressor ELF. Oncogene 25, 693–705.
Sasaki A, Masuda Y, Iwai K, Ikeda K, Watanabe K (2002). A RING finger protein Praja1 regulates Dlx5-dependent transcription through its ubiquitin ligase activity for the Dlx/Msx-interacting MAGE/Necdin family protein, Dlxin-1. J Biol Chem 277, 22541–22546.
Scaglione KM, Zavodszky E, Todi SV, Patury S, Xu P, Rodriguez-Lebron E, Fischer S, Konen J, Djarmati A, Peng J, *et al.* (2011). Ube2w and ataxin-3 coordinately regulate the ubiquitin ligase CHIP. Mol Cell 43, 599–612.
Schaffar G, Breuer P, Boteva R, Behrends C, Tzvetkov N, Strippel N, Sakahira H, Siegers K, Hayer-Hartl M, Hartl FU (2004). Cellular toxicity of polyglutamine expansion proteins: mechanism of transcription factor deactivation. Mol Cell 15, 95–105.
Shimohata T, Nakajima T, Yamada M, Uchida C, Onodera O, Naruse S, Kimura T, Koide R, Nozaki K, Sano Y, *et al.* (2000). Expanded polyglutamine stretches interact with TAFII130, interfering with CREB-dependent transcription. Nat Genet 26, 29–36.
Sowa AS, Martin E, Martins IM, Schmidt J, Depping R, Weber JJ, Rother F, Hartmann E, Bader M, Riess O, *et al.* (2018). Karyopherin alpha-3 is a key protein in the pathogenesis of spinocerebellar ataxia type 3 controlling the nuclear localization of ataxin-3. Proc Natl Acad Sci USA 115, E2624–E2633.
Stein TD, Anders NJ, DeCarli C, Chan SL, Mattson MP, Johnson JA (2004). Neutralization of transthyretin reverses the neuroprotective effects of secreted amyloid precursor protein (APP) in APPSW mice resulting in tau phosphorylation and loss of hippocampal neurons: support for the amyloid hypothesis. J Neurosci 24, 7707–7717.
Stenoien DL, Cummings CJ, Adams HP, Mancini MG, Patel K, DeMartino GN, Marcelli M, Weigel NL, Mancini MA (1999). Polyglutamine-expanded androgen receptors form aggregates that sequester heat shock proteins, proteasome components and SRC-1, and are suppressed by the HDJ-2 chaperone. Hum Mol Genet 8, 731–741.
Stork O, Stork S, Pape HC, Obata K (2001). Identification of genes expressed in the amygdala during the formation of fear memory. Learn Mem 8, 209–219.
Stoyas CA, La Spada AR (2018). The CAG-polyglutamine repeat diseases: a clinical, molecular, genetic, and pathophysiologic nosology. Handb Clin Neurol 147, 143–170.
Suhr ST, Senut MC, Whitelegge JP, Faull KF, Cuizon DB, Gage FH (2001). Identities of sequestered proteins in aggregates from cells with induced polyglutamine expression. J Cell Biol 153, 283–294.
Suzuki T, Raveau M, Miyake N, Sudo G, Tsurusaki Y, Watanabe T, Sugaya Y, Tatsukawa T, Mazaki E, Shimohata A, *et al.* (2020). A recurrent PJA1 variant in trigonocephaly and neurodevelopmental disorders. Ann Clin Transl Neurol 7, 1117–1131.
Tagawa K, Marubuchi S, Qi ML, Enokido Y, Tamura T, Inagaki R, Murata M, Kanazawa I, Wanker EE, Okazawa H (2007). The induction levels of heat shock protein 70 differentiate the vulnerabilities to mutant huntingtin among neuronal subtypes. J Neurosci 27, 868–880.

Tebbenkamp AT, Borchelt DR (2010). Analysis of chaperone mRNA expression in the adult mouse brain by meta analysis of the Allen Brain Atlas. PLoS One 5, e13675.
Theodoraki MA, Nillegoda NB, Saini J, Caplan AJ (2012). A network of ubiquitin ligases is important for the dynamics of misfolded protein aggregates in yeast. J Biol Chem 287, 23911–23922.
Thibaudeau TA, Anderson RT, Smith DM (2018). A common mechanism of proteasome impairment by neurodegenerative disease-associated oligomers. Nat Commun 9, 1097.
Trushina E, Heldebrant MP, Perez-Terzic CM, Bortolon R, Kovtun IV, Badger JD 2nd, Terzic A, Estevez A, Windebank AJ, Dyer RB, *et al.* (2003). Microtubule destabilization and nuclear entry are sequential steps leading to toxicity in Huntington's disease. Proc Natl Acad Sci USA 100, 12171–12176.
Tsai YC, Fishman PS, Thakor NV, Oyler GA (2003). Parkin facilitates the elimination of expanded polyglutamine proteins and leads to preservation of proteasome function. J Biol Chem 278, 22044–22055.
Tsvetkov AS, Arrasate M, Barmada S, Ando DM, Sharma P, Shaby BA, Finkbeiner S (2013). Proteostasis of polyglutamine varies among neurons and predicts neurodegeneration. Nat Chem Biol 9, 586–592.
Waelter S, Boeddrich A, Lurz R, Scherzinger E, Lueder G, Lehrach H, Wanker EE (2001). Accumulation of mutant huntingtin fragments in aggresome-like inclusion bodies as a result of insufficient protein degradation. Mol Biol Cell 12, 1393–1407.
Watabe K, Kato Y, Sakuma M, Murata M, Niida-Kawaguchi M, Takemura T, Hanagata N, Tada M, Kakita A, Shibata N (2020). Praja1 RING-finger E3 ubiquitin ligase suppresses neuronal cytoplasmic TDP-43 aggregate formation. Neuropathology 40, 570–586.
Wieland I, Weidner C, Ciccone R, Lapi E, McDonald-McGinn D, Kress W, Jakubiczka S, Collmann H, Zuffardi O, Zackai E, Wieacker P (2007). Contiguous gene deletions involving EFNB1, OPHN1, PJA1 and EDA in patients with craniofrontonasal syndrome. Clin Genet 72, 506–516.
Winslow AR, Chen CW, Corrochano S, Acevedo-Arozena A, Gordon DE, Peden AA, Lichtenberg M, Menzies FM, Ravikumar B, Imarisio S, *et al.* (2010). alpha-Synuclein impairs macroautophagy: implications for Parkinson's disease. J Cell Biol 190, 1023–1037.
Xiong B, Bayat V, Jaiswal M, Zhang K, Sandoval H, Charng WL, Li T, David G, Duraine L, Lin YQ, *et al.* (2012). Crag is a GEF for Rab11 required for rhodopsin trafficking and maintenance of adult photoreceptor cells. PLoS Biol 10, e1001438.
Ying Z, Wang H, Fan H, Zhu X, Zhou J, Fei E, Wang G (2009). Gp78, an ER associated E3, promotes SOD1 and ataxin-3 degradation. Hum Mol Genet 18, 4268–4281.
Yu P, Chen Y, Tagle DA, Cai T (2002). PJA1, encoding a RING-H2 finger ubiquitin ligase, is a novel human X chromosome gene abundantly expressed in brain. Genomics 79, 869–874.
Zoabi M, Sadeh R, de Bie P, Marquez VE, Ciechanover A (2011). PRAJA1 is a ubiquitin ligase for the polycomb repressive complex 2 proteins. Biochem Biophys Res Commun 408, 393–398.
Zoghbi HY, Orr HT (2000). Glutamine repeats and neurodegeneration. Annu Rev Neurosci 23, 217–247.